Contract No.:

This manuscript has been authored by Savannah River Nuclear Solutions (SRNS), LLC under Contract No. DE-AC09-08SR22470 with the U.S. Department of Energy (DOE) Office of Environmental Management (EM).

A Possible Oriented Attachment Growth Mechanism for Silver Nanowire Formation

Simona E. Hunyadi Murph[1]*
[1]*Savannah River National Laboratory*
Savannah River Site, Aiken, SC 29808

Catherine J. Murphy
[2]*University of Illinois at Urbana-Champaign*
Department of Chemistry
600 S. Mathews Ave., Urbana IL 61801

Austin Leach[3] *and Kenneth Gall*[3]
[3]*Department of Materials Science and Engineering*
Georgia Institute of Technology
Atlanta, GA 30332

**Corresponding author, email address: Simona.Murph@srnl.doe.gov*
Phone: 1-803-646-6761, Fax: 1-803-646-6761

Abstract

Electron microscopy studies suggest that silver nanowires prepared by an approach reported earlier by us (Caswell, K.K., Bender, C.M., Murphy, C.J. *Nano Lett.,* **2003***, 3,* 667-669) form through a coarsening process via an oriented attachment mechanism. Initially, silver nucleation centers were produced by chemical reduction of silver ions in boiling water, with sodium citrate and sodium hydroxide as additives in solution. These nucleation centers, with a twinned crystallographic orientation, ultimately merge into fully-grown silver nanowires. This is a completely different mechanism from the seed-mediated growth approach, which has also been used to produce silver nanowires. Companion molecular dynamics (MD) performed with the embedded atom method (EAM) are in agreement with our experimental data.

Introduction

One-dimensional metallic nanoparticles, such as nanowires, nanorods and nanotubes, are receiving considerable attention due to their distinctive optical, mechanical, catalytic and electronic properties.[1,2] One-dimensional nanoscale conductors are critical building blocks for nanoscale integrated circuits.[3]

The high level of current interest in one-dimensional nanomaterials has driven the scientific community to exploring a variety of innovative procedures for their production, including advanced nanolithographic techniques,[4-8] templating procedures in alumina or polymer membranes,[9] templating with carbon nanotubes,[10] and DNA,[11] etc. While these techniques can provide excellent tunability and control over the dimensions and physical placement of the final product, scaling up of these technologies is still hindered due to potentially tedious and expensive procedures. An alternative strategy for generating one-dimensional nanostructures is provided by wet chemical protocols, which might satisfy needs for cost-effective, large-scale manufacturing of nanomaterials.

Silver is the metal which exhibits the highest electrical and thermal conductivity,[12, 13] and could serve as interconnects between electronic circuits,[14] catalysts in chemical reactions[15-17] or substrates for surface-enhanced Raman spectroscopy.[18] High aspect ratios silver nanowires with uniform diameters were prepared by Xia's group via a self-seeding process that used poly(vinyl pyrrolidone) as the coordination reagent.[19-21] By using a seed-mediated approach, our group demonstrated the synthesis of one-dimensional nanostructures (gold and silver), with relatively high aspect ratios[22-24] using the structure-directing agent cetyltrimethylammonium bromide (CTAB).

Additionally, silver nanowires in an aqueous solution without any surfactant, polymer or even externally added seed crystallites were developed by our group.[25] In this procedure,

aqueous solutions of silver salt is reduced to silver metal by sodium citrate, at high temperatures (100 °C), in the presence of sodium hydroxide. Up to 20 microns long, but only 30 nm in diameter[25] silver nanowires are being produced by rigorous control of the hydroxide concentration. Preliminary electron diffraction data suggested a penta-tetrahedral twinned structure for these silver nanowires, similar to gold nanorods we had made earlier.[22-25] While a growth mechanism was not elucidated, we explained the formation of silver nanowires (as opposed to spheres, which are the product of analogous reactions with gold) as a result of preferential adsorption of ions to different crystal faces.[25] For example, it was plausible that the sodium citrate or hydroxide bound to the future side faces of the wires, {100} and {110}, permitting for the nanoparticles to grow along one dimension and produce five triangular {111} faces of silver at the wire ends.[25] Whether the binding affinity for these ions to different faces of silver would be the same, or not, at 100 °C, is an open question.

Molecular dynamics simulations of nanocrystal growth are rapidly appearing in the literature, and are helpful to interpret atomic-scale initial events in the nucleation and growth steps and guide experimental studies.[26-27]

Here we describe a high-resolution transmission electron microscopy (HRTEM) analysis of the creation of silver nanowires in aqueous solution, which shows a coarsening process via oriented attachment mechanism was followed in the growing process of silver nanowires. Electron microscopy studies suggest that torsional strain might twist and fuse small nanocrystals together. This growth mechanism is radically different from the seed-mediated methods we have proposed in the past,[21, 22, 28-32] and may suggest a reason why gold apparently does not undergo the same kind of process – gold nanorods in excess of 500 nm in length are uncommon in the literature, but silver nanowires with lengths of up to 20

μm are relatively common. Companion molecular dynamics (MD) performed with the embedded atom method (EAM) are in agreement with our experimental data. The atomistic simulation studies based on Voter's approach for face-centered cubic metallic silver with a pentagonal cross structure, particularly penta-twinned silver nanowires containing five (100) side faces and ends capped by five (111) faces with pentagonal cross-section along the common [110] axis, was used in this study.

Experimental Procedures

*Materials and Methods***.** Silver nitrate ($AgNO_3$, 99%), trisodium citrate (99%), and sodium hydroxide (NaOH, 99%) were from Sigma-Aldrich and used as received. Deionized ultra filtered water was used in our experiments. All glassware was cleaned with aqua regia and thoroughly rinsed with deionized ultra filtered water. High-resolution transmission electron microscopy data was performed on JEM-2100F with illumination system Cs corrector and a Hitachi 8000 transmission electron microscope operating at 200kV. An Eppendorf centrifuge model 5418 was used to centrifuge our samples.

Synthesis of Ag Nanowires. Silver nanowires were prepared as previously described.[25] At the beginning, two aqueous solutions, A and B, were prepared in two separate 250 mL conical flasks. Two separate 50 mL beakers were used as lids. 1.5 μL of 1 M aqueous NaOH and 40 μL of 0.1 M aqueous $AgNO_3$ were added to 100 mL deionized water (Solution A).. This aqueous solution was brought to a boil for ~5 minutes while rapidly stirring. The second solution (Solution B) containing 150 mL deionized water, 1.5 μL of 1 M aqueous NaOH, and 20 μL of 0.1 M aqueous $AgNO_3$, was also prepared. 5 mL of aqueous 0.01 M trisodium citrate was added to a boiling Solution A. This mixture was refluxed for 10 minutes. A 2 μL

aliquot of this solution was removed from the solution TEM analysis. After that, Solution A and Solution B were refluxed at 100°C for one hour. Every 5-10 minutes, 2 μL of this solution were sampled and placed on a copper TEM grid for subsequent TEM imaging. The silver nanowires produced here were purified by centrifugation (7000 rpm for 10 minutes).

Results and Discussion

Transmission Electron Microscopy Study of Silver Nanowire Growth

The preparation of silver nanowires starts with chemical reduction of silver ions in boiling water, with sodium citrate and sodium hydroxide as additives in solution. Silver nanowires with the following dimensions were produced by this method: 30 ± 3 nm in diameter and a highly variable length (200 nm to 20 μm long). In previous work we had only examined the morphology of the final product, at t = 60 minutes.[25] Transmission electron microscopy was employed to record and evaluate intermediate steps in the evolution of silver nanowires (Figure 1). At t = 10 minutes, irregular and non-uniform silver nanoparticles with 90 ± 27 nm diameters were prepared (Solution A) (Figure 1a). As more aqueous solution containing silver nitrate and sodium hydroxide (Solution B) was added to this solution, additional "nucleation centers" were formed at the expense of the initial 90 ± 27 nm spherical particles. When analyzed, these nucleation centers were uniform in size with a diameter of 11±1 nm.

Typical images shown in Figure 1b, c, d for t = 5 minutes reveal that, in the early stages of the reaction, these spherical Ag nucleation centers align in a surprisingly ordered fashion and resulted in the development of long stripes. The formation of these stripes, reminiscent of a "beads on a string" configuration, was observed all over the grid repeatedly. The distance between the small Ag nanoparticles is significant, from ~1-3 diameters apart.

In this TEM instrument, the resolution is ~3 nm; therefore, sub-3-nm Ag clusters might be in between the more easily-visualized particles as linkers. As the boiling continues, a coarsening process takes place in between the neighboring Ag nucleation centers and through an oriented attachment mechanism the particles aggregate into short rods (t = 20, 30, 40 minutes; Figure 1e, f, g) , and ultimately silver nanowires.

Figure 2 shows the proposed schematic growth mechanism of silver nanostructures and nanowires. At the beginning of the reaction, the irregular silver nanoparticles were produced when sodium citrate was added to an aqueous boiling solution of silver nitrate. The oxidation potential of citrate is +0.19V compared to the Ag^{+}/Ag reduction potential of +0.8 V (at room temperature).[33] At this point, citrate is likely to be capping the nanoparticles. Next, addition of aqueous solution of more silver ions and sodium hydroxide result in much smaller nanoparticles, 11 ± 1 nm in diameter compared to the original 90 ± 9 nm diameter irregular nanoparticles. It is unclear at this point why the 90 ± 9 nm diameter nanoparticles decreased in size after addition of aqueous solution of more silver ions and sodium hydroxide. We can only assume that at 100^{o}C, which is the temperature of reaction, sodium citrate is partially removed from different faces and possible replaced by hydroxide ions; this will results in a decrease in size of the nanoparticles. The electrochemical reaction that takes place here is based on two processes: metal oxidation and reduction of the oxidizer.[34] While O_2 can act as an oxidant for silver[35] it is unclear if this is the case for our specimen or if the OH^{-} act as a coordinating ligand. As the reaction proceeds at 100˚C, these 11 nm nanoparticles collide and fuse to form the nascent nanowires – assuming that what we observe on the TEM grid is representative of what happens in solution. The growing process takes places as more

particles collide and form larger nanostructures via an oriented attachment mechanism (see below).

This general idea is similar to the work reported by Banfield for the crystal growth of mercaptoethanol-capped nanocrystalline ZnS by hydrothermal coarsening.[36] The coarsening and oriented attachment processes, which are temperature dependent processes, were credited to ligand's removal and surface reorganization and Ostwald ripening. [30,36-38] They also reported an enhanced Brownian motion of the water molecules present in the close proximity of the nanoparticle's surface which could induce repositioning and rearrangement of nanocrystals in solution.[36-38]

Oriented attachment could be described as a self-directed arrangement of neighboring nanoparticles when particles with identical crystallographic configurations are present. When the crystallographic orientation is encountered, these nanoparticles merge together.[37,38] This favorable process reduces the overall surface energy due to the elimination of energy associated with unsatisfied bonds. This process has been demonstrated for the fabrication of titania nanoparticles. [37,38]

Our results, even if somewhat counterintuitive, are also in agreement with the oriented-aggregation high-resolution electron microscopy studies reported by Liz-Marzan.[39] Silver nanowires were prepared at high temperatures in the presence of poly(vinylpyrolidone) (PVP) by solvent reduction in N, N-dimethylformamide (DMF). Their HRTEM images demonstrate that silver crystalline nanowires were produced when icosahedral and cuboctahedral Ag nanoparticles (that formed initially in the reaction pot) self-assembled and fused together. However, in their case, the polymer could presumably

align nanoparticles initially. In our experiments, “nothing” is holding the 11 nm nanoparticles in a line, unless smaller ones, below the resolving power of the TEM, are present.

La Mer principle could be used to describe the nucleation and growth silver nanowires.[40] This mechanism suggests that two different processes are predominant during the formation of colloids from a homogeneous medium. Initially, when thermodynamic and kinetic parameters are met, a short burst of nucleation occurs until the silver atoms get to a supersaturation point. Once the supersaturation point is met, the Ag atoms start to nucleate into small nuclei centers. Once formed, these nuclei grow rapidly forming larger clusters resulting in a concentration drop of metal atoms. As expected, this will reduce the concentration of atoms available for further nucleation which will limit future nucleation events. Continuous supply of atoms produced in the reaction leads to larger size nanocrystals. An equilibrium is finally achieved when the atoms on the surface of the nanocrystal equals the atoms in the solution.

A closer inspection of the nucleation centers by HRTEM reveals a penta-twinned crystallographic structure with five well-defined facets typical for an icosahedra structures (we assume that these nucleation centers are icosahedra) (Figure 3). These results are reflected also in Fourier transform diffraction pattern which projects double spot arrays but with a uniform and regular distribution (Figure 3d). An analysis performed on the Ag nucleation centers allowed us to determine that the spacings between the pentatwinned fringes of the specimen. These results suggest that fringes centers matches (111) orientation of silver crystal with a fcc arrangement.

A detailed HRTEM study allowed us to monitor the coarsening process in the intermediate stages before the nanowires were formed (Figure 4) at time t = 5 minutes (A+B

solutions). The low-resolution TEM can not capture the presence of the small 3 ± 2 nm Ag nanoparticles (Figure 4) present in between the nucleation centers (11 ± 1nm). The HRTEM image (Figure 4a) shows the presence of this 3±2 nm that can act as a template and can further determine the oriented attachment growth of the nano-centers. At the beginning, the process is initiated by an organized alignment of the silver nucleation centers (11 ± 1nm) due to the agglomeration of 3±2 nm particles. Next, the coarsening process takes place probably when favorable crystallographic facets are facing each other.

Synthesis and Characterization of Fully-Grown Silver Nanowires

Silver nanowires were produced after boiling aqueous solutions of silver nitrate in the presence of sodium hydroxide and sodium citrate for 50-60 minutes. Our results show that the diameter of the particles is ~ 30 ± 3 nm with a length that varies from 200 nm up to 20 microns.[18, 25, 41]

The formation of silver nanowires can be easily visualized when the solution turned pale yellow.[35] Silver nanowires have a transverse plasmon band at ~400 nm and a longitudinal band in the near-infrared area.[18, 25]

Diffraction patterns along with the high-resolution transmission electron microscopy (HRTEM) (Figure 5) performed on the silver nanowires suggests a twinned crystallographic orientation structure. HRTEM images show well-organized and distributed paired atom arrangements that are aligned in the direction of elongation to the Ag nanowire. This is in agreement with the crystallographic arrangement of the nucleation centers and implies that the original crystallization structure is responsible for the final crystallization organization.

Molecular statics simulations at 0K were used to determine a few different equilibrium wire structures. Wires were constructed with atoms in the FCC positions and

then relaxed in a static framework to minimum energy. Low energy configurations are shown here. Simulations on the silver nanowires reveal that the direction of evolution and growth of Ag nanowires is [100]. A combination of different faces, Ag {100} or Ag {110}, or both were observed. Penta-twinned surfaces, in the form of five Ag {111} triangular faces were documented on the tip of the nanowires.[42,43] Figure 6 shows a low energy configuration where the growth direction of the nanowire maintains low energy {111} surfaces while the sides are higher energy {100} and {110} surfaces. A penta twinned internal structure enables low energy joining of the five atomic wedges with set surface and favorable {111} growth planes. Figure 6 and figure 7 shows an alternative pentagonal wire structure where the wire surface contains {111} facets, which minimize overall wire energy without regard for formation mechanism. The simulations confirm the five fold twins observed inside the wires. However, the simulations do not consider the attachment of surfactants or the kinetics of growth and thus cannot predict the exact surface structure on the long sides of the wires.

Ultrafine single-crystalline gold nanowires were also created by an oriented attachment approach in Halder's group.[44] Preferential removal of the surfactant, e.g. amine, from the {111} planes of the nanoparticles followed by nanoparticle fusion resulted in the creation of Au wires. This is not surprising since different facets denote different surface energies and different binding energies on the nanoparticle's surface.[44]

Gold nanowires prepared in the presence of structure-directing agents, e.g. cetyltrimethylammonium bromide,[45-47] oleylamine,[48] polyvinylpyrrolidone (PVP),[49] have been reported by us and others. In these cases, the growth mechanism is based on either a seed-mediated method which produces gold nanorods/nanowires up to ~ 600 nm long[45-46], and/or structure directing agents;[48-49] whereas silver nanowires up to ~20 microns long are

reachable via the citrate reduction/oriented attachment approach.[25] The citrate reduction method was also employed for the synthesis of colloidal gold. However, reduction of $AuCl_4^-$ to Au atoms produces only spherical gold nanoparticles. Isotropic and anisotropic gold nanoparticle formation have been the topic of many scientific papers.[50, 51] In a recent paper, Doyen et al suggests that citrate behaves as a "molecular linker" between Au(I) and/or Au(0) atoms, assisting in the formation of gold nanoparticles.[51] A close investigation of this method for producing colloidal Au has revealed that Au nanoclusters of about 5 nm in diameter are being produced at the beginning of the reaction.[52] These small Au nanoclusters aggregate in a widespread network of nanowires. Once additional Au atoms are produced, they attach to the nanowire grids already in place, leading to larger diameter Au networks. Apparently, the increase in diameter destabilizes the nanowires, which fragment and cleave into sphere-like particles. The nanowires were inherently unstable in the reaction and quickly converted to the spherical particles, but can be conveniently harvested by quenching the reaction with rapid cooling. [52]

Palladium polycrystalline nanowires produced in ethylene glycol (EG)–dimethyl sulfoxide (DMSO)[53] or tetraoctadecylammonium bromide[54] have also reported. Heterogeneities in surface charge and polarity associated with the nonuniform spatial distribution of surfactant on different crystal facets is possibly the driving force for anisotropic self-assembly in these cases.[53]

Other workers have examined other inorganic nanoparticle systems that make one-dimensional materials via oriented attachment. Giersig found that crystalline nanowires CdTe can be produced by the targeted removal of the organic surfactant (thioglycolic acid) with ethanol present of the quantum dots surface.[55] A strong dipole-dipole interaction between the

quantum dots along with a spontaneously self-(re)organization via an oriented arrangement produces one dimensional nanostructures. However, a CdTe nanoparticle has a net dipole and is not clear that Ag would.

A dipole-dipole attraction might be possible due to a preferential crystallographic attachment of ions on the surfaces of nanoparticles.[39] Pileni suggests that hydroxide ions can also function as a structure-directing surfactant while promoting anisotropic growth of nanoparticles crystals.[57,58] An oriented attachment growth mechanism was also used to describe the production of PbSe nanowires in solution.[59] Single crystal lattice nanowires were produced by an oriented attachment when {100}, {110}, or {111} faces fused together in the presence of different surfactants.[59] Weller reported the formation of one-dimensional ZnO nanostructures from spherical nanostructures due to the enhanced reactivity of [002] planes within wurzite arrangement.[56]

One could tailor nanoparticles' shape by taking into account the specific surface energies of crystal planes. According to Wulff's facets theory,[55] when the equilibrium conditions are met, a crystal has to meet the minimum surface energy. As a result, the shape of the nanoparticles determines the fundamental symmetry of the corresponding lattice.[60] According to the Ostwald ripening process and growth kinetic mechanism, larger particles grow at the expense of smaller particles, because larger crystals are more energetically stable than smaller ones.[61]

The interactions between adjacent nanoparticles, including Coulombic interactions, van der Waals interactions, and dipolar interactions have to be taken into account when discussing the oriented attachment mechanism.[62] The Coulombic interactions are predominant when nanoparticles in solution are adjacent to each other. However, when two

particles are far apart in a solution, van der Waals interactions are the main forces driving the oriented attachment process.[62] Moreover, a recent study[53] shows that van der Waals interactions are highly dependent on the nanoparticle's morphology, geometry (size, aspect ratio) and also the inter-nanoparticle separation during the oriented-attachment growth of one-dimensional nanoparticles.[63] The oriented attachment growth mechanism of nanoparticles is affected by the solution conditions, solvent selection, dielectric constant, pH among others.[64], [65]

Our experimental and model data in corroboration with data reported by others suggest that the nanowire crystal growth is a complex process that may by more than one mechanism simultaneously via an oriented attachment and coarsening.

Conclusion

An important conclusion from this study is that oriented attachment and growth can lead to the formation of silver nanowires with twinned crystallographic structures. This comes as a result of a coarsening process via oriented attachment mechanism of the penta-twinned crystallographic structure of the nucleation centers, which will fuse and produce silver nanowires.

References:

1. Xia, Y.; Yang, P.; Sun, Y.; Wu, Y.; Mayers, B.; Gates, B.; Yin, Y.; Kim, F.; Yan, H. *Adv. Mater.* **2003**, 15, 353 – 389.

2. Feldheim, D. L., Foss, C. A., Jr., Eds. *Metal Nanoparticles: Synthesis, Characterization and Applications*; Marcel Dekker: New York: **2002**.

3. Huang, Y.; Duan, X. F; Wei, Q. Q.; Lieber, C. M., *Science* **2001**, 291, 630-633.

4. Cerrina, F.; Marrian, C. *MRS Bull.* **1996**, 21, 56-62.

5. Gibson, J. M. *Phys. Today* **1997**, 50, 56-61.

6. Matsui, S.; Ochiai, Y. *Nanotechnology* **1996**, 7, 247-258.

7. Hong, S. H.; Zhu, J.; Mirkin, C. A. *Science* **1999**, 286, 523-525.

8. Dagata, J. A. *Science* **1995**, 270, 1625-1626.

9. Martin, C. R. *Science* **1994**, 266, 1961-1966.

10. Ugarte, D.; Châtelain, A.; de Heer, W. A. *Science* **1996**, 274, 1897-1899.

11. Braun, E.; Eichen, Y.; Sivan, U.; Ben-Yoseph, G. *Nature* **1998**, 391, 775-778.

12. Bhattacharyya, S.; Saha, S. K.; Chakravorty, D. *Appl. Phys. Lett.* **2000**, 77, 3770-3772.

13. Gao, H.; Murphy, C. J.; Caswell, K. K. *NanoLett.* **2003**, 3, 1495-1498.

14. Hu, J.; Odom, T. W.; Lieber, C. M. *Acc. Chem. Res.* **1999**, 32, 435-445

15. Chimentão, R. J.; Medina, F.; Fierro, J. L. G.; Sueiras, J. E.; Cesteros, Y.; Salagre, P. *J. Molec. Catalysis A-Chemical* **2006**, 258, 346-354.

16. Wei, Q.; Li, B.; Li, C.; Wang, J.; Wang, W.; Yang, X. *J. Mater. Chem.* **2006**, 36, 3606-3608.

17. Tominaga, M.; Shimazoe, T.; Nagashima, M.; Kusuda, H.; Kubo, A.; Kuwahara,Y.; Taniguchi, I. *J. Electroanal. Chem.* **2006**, 590, 37-46.

18. Hunyadi, S. E.; Murphy, C. J., *J. Mater. Chem*. **2006**, 16, 3929 – 3935 and references herein.

19. Sun, Y.; Gates, B.; Mayers, B.; Xia, Y. *Nano Lett.* **2002**, 2, 165-168.

20. Sun, Y.; Xia, Y. *Adv. Mater.* **2002**, 14, 833-837.

21. Sun, Y.; Yin, Y.; Mayers, B. T.; Herricks, T.; Xia, Y. *Chem. Mater*. **2002**, 14, 4736-4745.

22. Jana, N. R.; Gearheart, L. A.: Murphy, C. J. *Chem. Commun.* **2001**, 617-618;

23. Murphy, C. J.; Jana, N. R. *Adv. Mater.* **2002**, 14, 80-82.

24. Jana, N. R.; Gearheart, L. A.; Murphy, C. J. J. *Phys. Chem. B* **2001**, 105, 4065-4067.

25. Caswell, K. K., Bender, C. M., Murphy, C. J. *Nano Lett.* **2003**, 3, 667-669.

26. Fichthorn, K. A. *Molecular Simulation* **2014**, 40, 134–140.

27. Zhou, Y., Fichthorn, K. *J. Phys. Chem. C* **2014**, 118, 18746−18755.

28. Murphy, C. J.; San, T. K.; Gole, A. M.; Orendorff, C. J.; Gao, J. X.; Gou, L.; Hunyadi, S. E.; Li, T. J. *Phys. Chem.* B **2005**, 109, 13857-13870.

29. Murphy, C. J.; Gole, A. M.; Hunyadi, S. E.; Orendorff, C. J. *Inorg. Chem.* **2006**, 45,

7544-7554.

30. Johnson, C. J.; Dujardin, E.; Davis, S. A.; Murphy, C. J.; Mann, S. *J. Mater. Chem*. **2002**, 12, 1765-1770.

31. Sau, T. K.; Murphy, C. J. *J. Am. Chem. Soc.* **2004**, 126, 8648-8649.

32. Jana, N. R.; Gearheart, L.; Murphy, C. J. *Adv. Mater.* **2001**, 13, 1389-1393.

33. Milazzo, G., Sharma, V.K., Caroli, S. *Tables of Standard Electrode Potentials* Wiley, New York, NY, **1978.**

34. Xia, Y.; Zhao, X. M.; Kim, E.; Whitesides, G. M. *Chem. Mater.* **1995**, 7, 2332-2337.

35. Xia, Y.; Kim, E.; Whitesides, G. M., *J. Electrochem. Soc.* **1996**, 143, 1070-1079.

36. Huang, F.; Zhang, H.; Banfield J. F. *Nanolett.* **2003**, 3, 373-378.

37. Penn, R. L.; Banfield, J. F. *American Mineralogist* **1998**, 83, 1077-1082.

38. Penn, R. L.; Banfield, J. F. **Scienc**e 281, 969-971.

39. Giersig, M.; Pastoriza-Santos, I.; Liz-Marzan, L. M. *J. Mater. Chem.* **2004**, 14, 607-610.

40. Tao, A. R.; Habas, S.; Yang, P. *Small* **2008**, 4, 310 – 325.

41. Hunyadi, S. E.; Murphy, C. J. *J. Phys. Chem. B* **2006**, 110, 7226 -7231.

42. Lucas, M.; Leach, A. M.; McDowell, M. T.; Hunyadi, S. E.; Gall, K.; Murphy, C. J.; Riedo, E. *Physical Review B* **2008**, 77, 2454201-2452014.

43. Tao, C. G.; Cullen, W. G.; Williams, E. D.; Hunyadi, S. E.; Murphy, C. J., *Surface Science* **2007**, 601, 4939- 4943.

44. Halder, A.; Ravishankar, N. *Adv. Mater*. **2007**, 19, 1854-1858.

45. Murphy, C. J.; Gole, A. M.; Hunyadi, S. E.; Orendorff, C. J., *Inorg. Chem.* (Forum Article) **2006**, 45, 7544-7554.

46. Murphy, C. J.; Sau, T. K.; Gole, A. M.; Orendorff, C. J.; Gao, J.; Gou, L.; Hunyadi, S. E., Li, T. *J. Phys. Chem. B* **2005**, 109, 13857-13870.

47. Critchley, K.; Khanal, B. P.; Gorzny, M. L.; Vigderman, L.; Evans, S. D.; Zubarev, E. R.; Kotov, N. A. *Adv. Mater.* **2010**, 22, 2338-2342.

48. Chen, Y.; Ouyang, Z.; Gu, M.; Cheng, W. *Adv.Mater.* **2013***,* 25, 80–85.

49. Navaladian, S.; Janet, C. M.; Viswanathan, B.; Varadarajan, T. K.; Viswanath, R. P. *J. Phys. Chem. C* **2007**, 111, 14150-14156.

50. Thanh, N.T. K.; Maclean, N.; Mahiddine S. *Chem. Rev.* **2014**, 114, 7610−7630 and references herein.

51. Doyen, M.; Bartik, K.; Bruylants, G. *J. Coll. Inter. Science* **2013**, 399, 1–5.

52. Pong, B. K.; Elim, H. I.; Chong, J. X.; Ji, W.; Trout, B. L.; Lee, J. Y. *J. Phys. Chem. C* **2007**, 111, 6281-6287.

53. Taratula, O.; Chen, A. M.; Zhang, J.; Chaudry, J.; Nagahara, L.; Banerjee, I.; He, H. *J. Phys. Chem. C* **2007**, 111, 7666-7670.

54. Feng, C.; Zhang, R.; Yin, P.; Li, L.; Guo, L.; Shen, Z. *Nanotechnology* **2008**, 19, 305601-305609.

55. Tang, Z.; Kotov, N. A.; Giersig, M. *Science* **2002**, 297, 237 – 240.

56. Pacholski, C.; Kornowski, A.; Weller, H.; *Angew. Chem. Int. Ed.* **2002**, 41, 1188-1191.

57. Filankembo, A.; Pileni, M. P. *J. Phys. Chem. B* **2000**, 104, 5865-5868.

58. Filankembo, A.; Giorgio, S.; Lisiecki, I.; Pileni, M. P. *J. Phys. Chem. B* **2003**, 107, 7492-7500.

59. Cho, K. S.; Talapin, D. V.; Gaschler, W.; Murray, C. B. *J. Am. Chem. Soc.* **2005**, 127, 7140.

60. Zhang, Q.; Liu, S. J.; Yu, S. H. *J. Mater. Chem*. **2009**, 19, 191–207.

61. Sugimoto, T. *Adv. Colloid Interface Sci*. **1987**, 28, 65.

62. Zhang, H.; Banfield, J.F. CrystEngComm, 2014, 16, 1568-1578.

63. Lv, W.; Yang, X.; Wang, W.; Niu, Y.; Liu, Z.; He, W. *ChemPhysChem* **2014**, 15, 2688–2691.

64. Burrows, N. D.; Hale, C. R. H.; Penn, R. L. *Cryst. Growth Des.* **2013**, 13, 3396−3403.

65. Burrows, N.D.; Kesselman, E.; Sabyrov, K.; Stemig, A.; Talmonb, Y.; Penn, R.L. *CrystEngComm* **2014**, 16, 1472-1481.

For Table of Contents Use Only

A Possible Oriented Attachment Growth Mechanism for Silver Nanowire Formation

Simona E. Hunyadi Murph[1, 2]*
[1]*Savannah River National Laboratory*
Savannah River Site, Aiken, SC 29808

[2]*Georgia Regents University*
Department of Chemistry and Physics
2500 Walton Way, Augusta, GA 30901

Catherine J. Murphy[3]
[3]*University of Illinois at Urbana-Champaign*
Department of Chemistry
600 S. Mathews Ave., Urbana IL 61801

Austin Leach[4] *and Kenneth Gall*[4]
[4]*Department of Materials Science and Engineering*
Georgia Institute of Technology
Atlanta, GA 30332

**Corresponding author, email address: Simona.Murph@srnl.doe.gov*
Phone: 1-803-646-6761, Fax: 1-803-646-6761

Figure 1. Growth mechanism of silver nanowires solution A (a), and solution A+ B after boiling 5 minutes (b, c, d), 10 minutes (e), 20 minutes (f), 30 minutes (g) and 40 minutes (h), respectively. After 40 minutes the amount of spherical Ag nanoparticles is drastically reduced, leaving behind silver nanowires and ~5% spherical particles. Scale bar: 500 nm a-g, 2 microns-h.

Figure 2. Schematic illustration of the coarsening mechanism via oriented attachment process for the evolution of silver into one-dimensional nanostructures. Solution A: (i) 10 minutes boiling, Solution A+B after boiling (ii) 5, (iii) 10, (iv) 20, (v) 40, or (vi) 60 minutes; as the boiling proceeds, from 5 minutes up to 60 minutes, the "nucleation centers" merge together and form silver nanowires.

Figure 3. (a, b, c) HRTEM on the 11 nm nucleation centers. A five fold penta-twinned crystallographic structure is observed. (d) Diffraction pattern recorded on the nucleation centers that suggest support the HRTEM regarding the penta-twinned crystallographic structure. The distance between the fringes in this case indicate (111) faces.

Figure 4. (a) HRTEM on nucleation centers in the coarsening process via an oriented attachment mechanism; (b) An HRTEM image of two fused particles with favorable crystallographic orientations. Scale bar: 2 nm - a, 5 nm - b.

Figure 5. (a, b, c, d, e) High resolution TEM images on silver nanowires prepared by a seedless, surfactantless method along with the (f) diffraction pattern. This suggests a staking fault of (110) or other faces of the Ag nanowires with a pentatetrahedral twin orientation.

Figure 6. Equilibrium atomic positions for a pentagonal nanowire with internal twins.

Figure 7. Equilibrium atomic positions for a smaller pentagonal nanowire and a pentagonal wire with {111} surfaces.

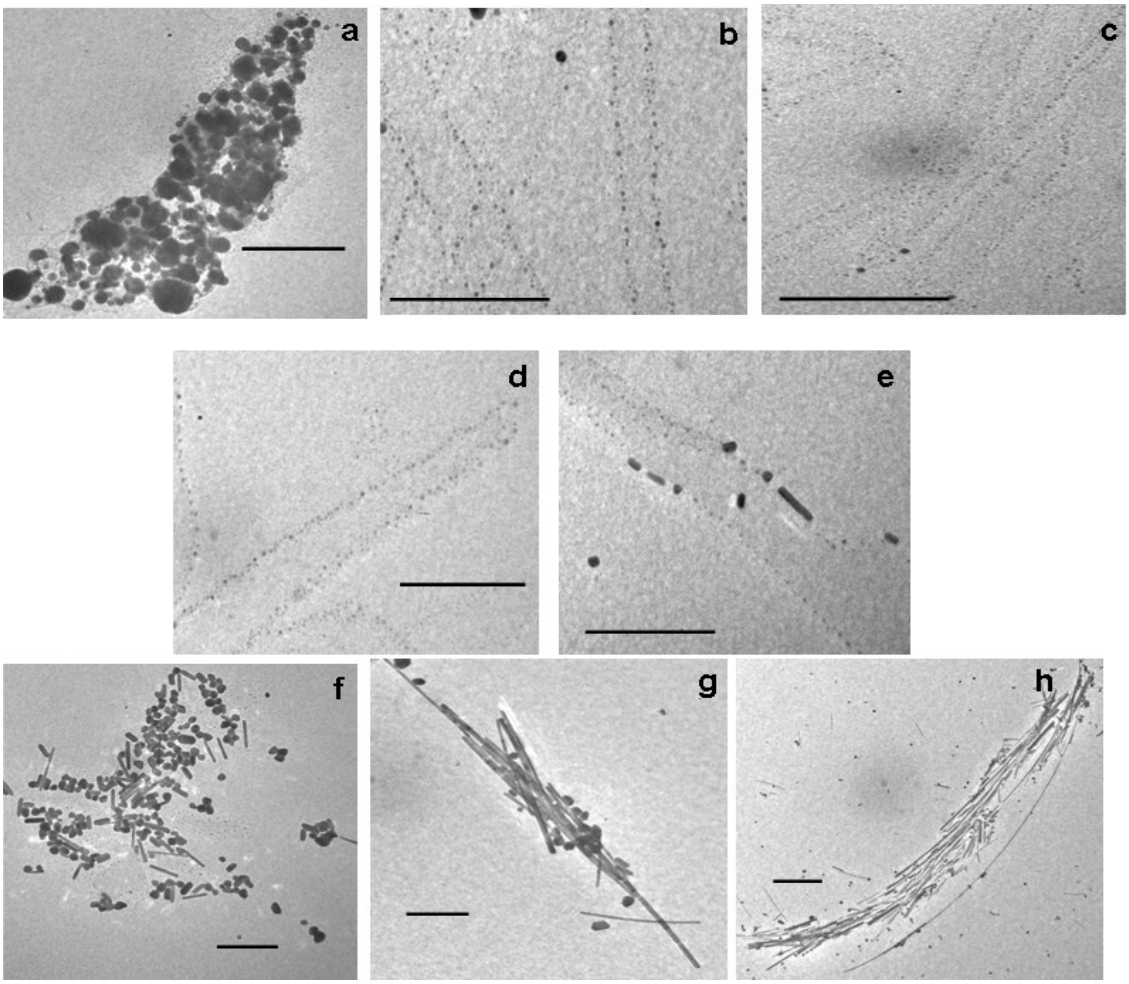

Figure 1. Growth mechanism of silver nanowires solution A (a), and solution A and B after boiling 5 minutes (b, c, d), 10 minutes (e), 20 minutes (f), 30 minutes (g) and 40 minutes (h), respectively. After 40 minutes the amount of spherical Ag nanoparticles is drastically reduced, leaving behind silver nanowires and ~5% spherical particles. Scale bar: 500 nm a-g, 2 microns-h.

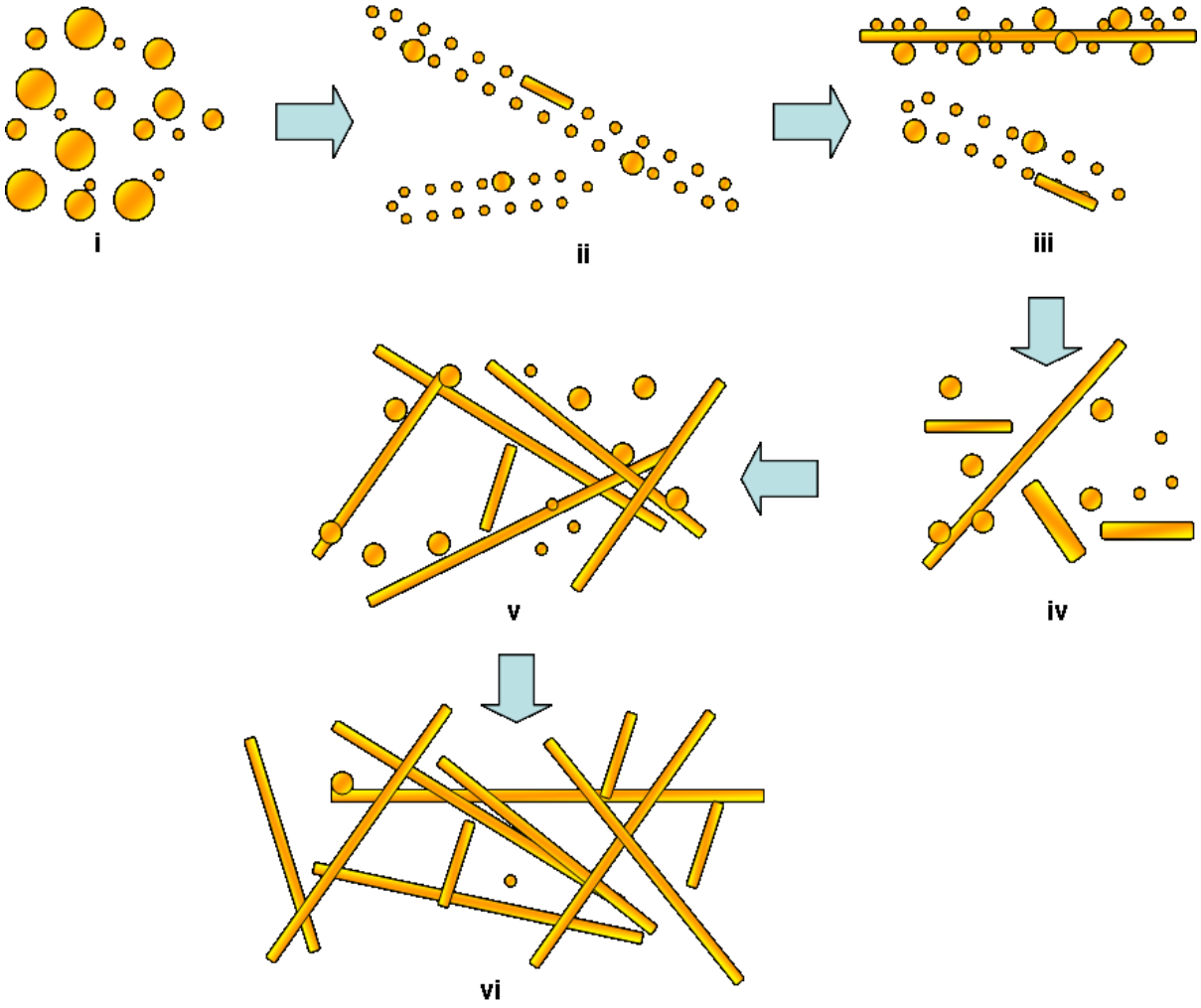

Figure 2. Schematic illustration of the coarsening mechanism via oriented attachment process for the evolution of silver into one-dimensional nanostructures. Solution A after (i) 10 minutes boiling containing different sizes of Ag spherical nanoparticles, 90±27nm, Solution A+B after boiling (ii) 5 minutes, (iii) 10 minutes, (iv) 20 minutes, (v) 40 minutes, (vi) 50-60 minutes, containing uniform spherical "nucleation centers"; as the boiling proceeds, from 5 minutes up to 60 minutes, these "nucleation centers" merge together and form silver nanowires.

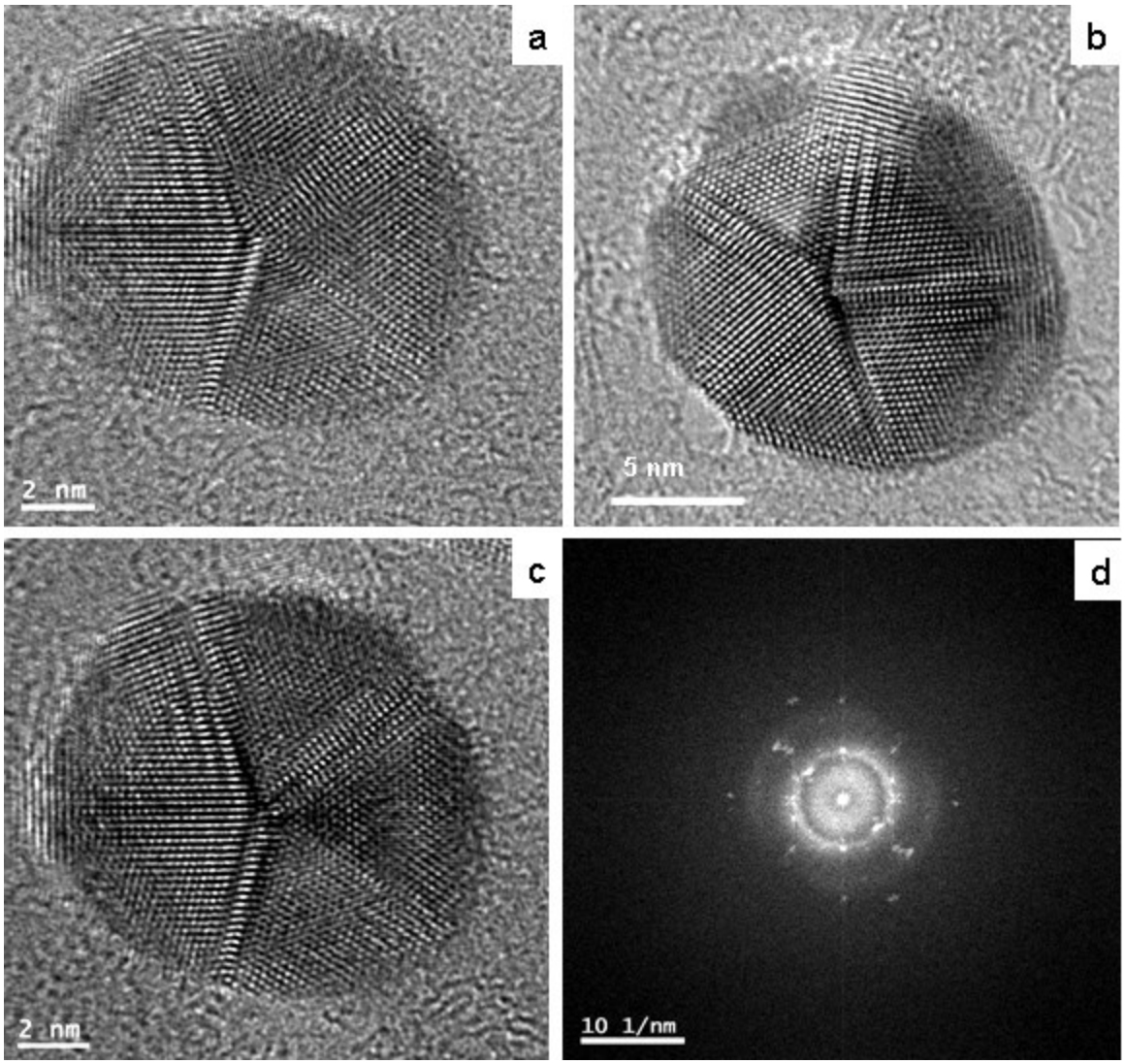

Figure 3. (a, b, c) HRTEM on the 11 nm nucleation centers. A five fold penta-twinned crystallographic structure is observed. (d) Diffraction pattern recorded on the nucleation centers that suggest support the HRTEM regarding the penta-twinned crystallographic structure. The distance between the fringes in this case indicate (111) faces.

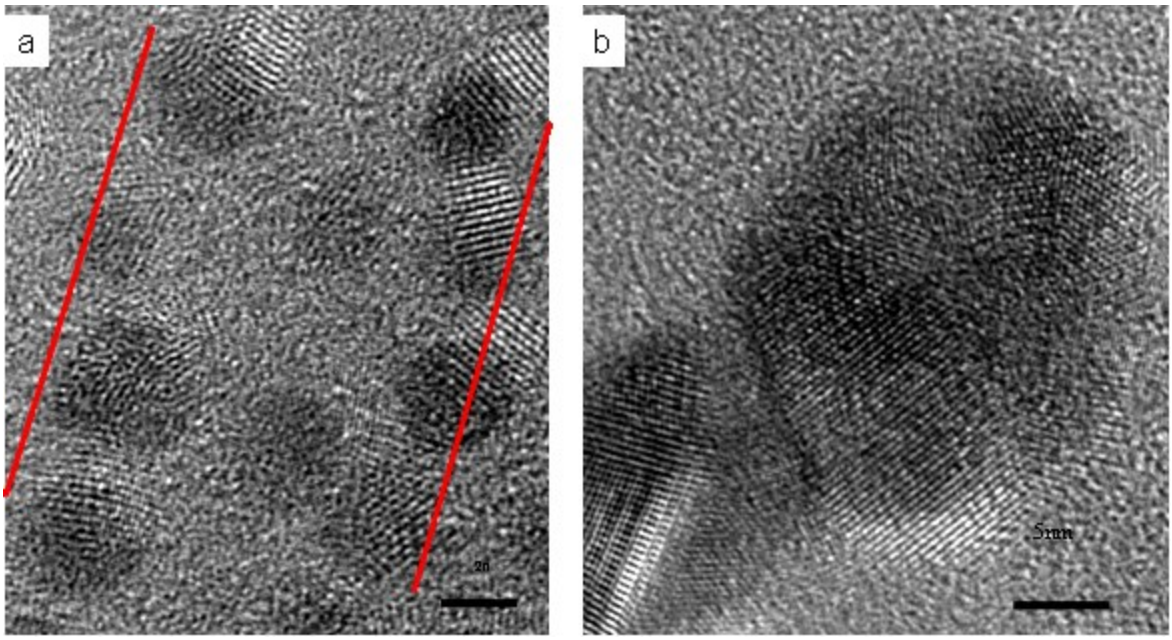

Figure 4. (a) HRTEM on nucleation centers in the coarsening process via an oriented attachment mechanism; (b) An HRTEM image of two fused particles with favorable crystallographic orientations. Scale bar: 2 nm - a, 5 nm - b.

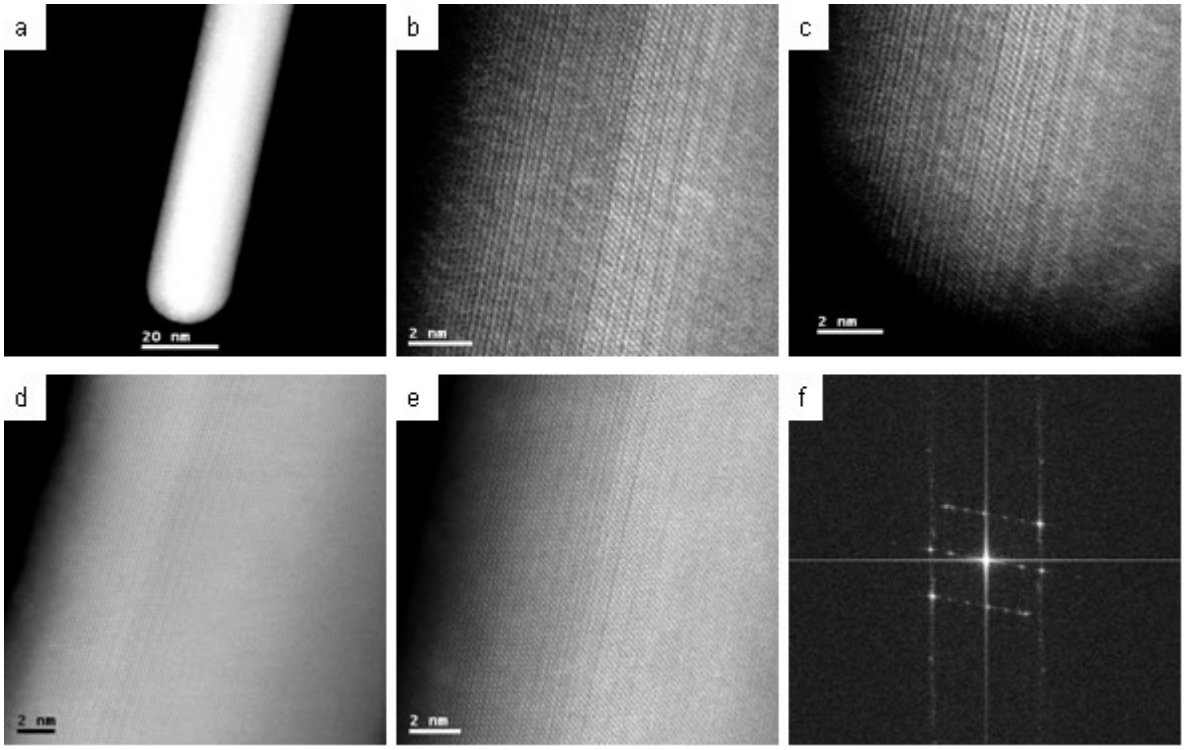

Figure 5. (a, b, c, d, e) High resolution TEM images on silver nanowires prepared by a seedless, surfactantless method along with the (f) diffraction pattern. This suggests a staking fault of (110) or other faces of the Ag nanowires with a pentatetrahedral twin orientation.

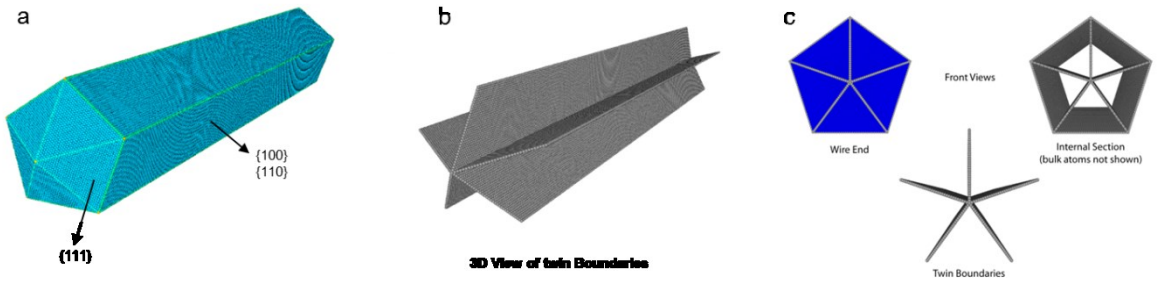

Figure 6. Equilibrium atomic positions for a pentagonal nanowire with internal twins.

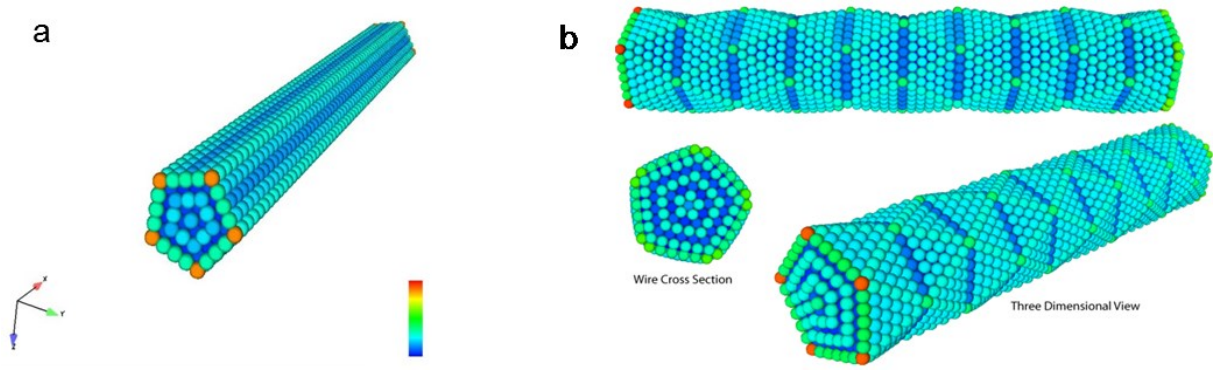

Figure 7. Equilibrium atomic positions for a smaller pentagonal nanowire and a pentagonal wire with {111} surfaces.